Published by Avanti Publishers

International Journal of Petroleum Technology

ISSN (online): 2409-787X

Prediction of Petrophysical Properties using Post Stack Seismic Inversion and Geostatistical Techniques over F-3 Block, Netherlands - A Comparative Study

Prabodh K. Kushwaha[1], Raghav Singh[1], Satya P. Maurya[1,*] and Piyush Rai[2]

[1]*Department of Geophysics, Institute of Science, Banaras Hindu University, Varanasi-221005, India*

[2]*Department of Mining Engineering, Indian Institute of Technology (BHU), Varanasi-221005, India*

ARTICLE INFO

Article Type: Research Article

Academic Editor: Ahmed N. Al-Dawood

Keywords:
P-impedance
Seismic Inversion
Model Based Inversion
Probabilistic Neural Network
Multi-Layer Feed Forward Network

Timeline:
Received: July 05, 2023
Accepted: August 09, 2023
Published: September 22, 2023

Citation: Kushwaha PK, Singh R, Maurya SP, Rai P. Prediction of petrophysical properties using post stack seismic inversion and geostatistical techniques over F-3 block, Netherlands - A comparative study. Int J Petrol Technol. 2023; 10: 53-70.

DOI: https://doi.org/10.15377/2409-787X.2023.10.5

ABSTRACT

To estimate petrophysical parameters, seismic inversion techniques have been frequently used for estimating attributes like P-impedance, elastic impedance, S-impedance, density, V_P / V_S ratio, and gamma-ray logs from seismic and well-log data. These characteristics enable us to comprehend subsurface lithology for geo-seismic analysis, including its extent and shape. Four different post-stack inversion techniques, including bandlimited inversion (BLI), colored inversion (CI), maximum likelihood sparse spike inversion (MLSSI), and model-based inversion (MBI), have been applied to the post-stack seismic data from the F3 block in the Netherlands in this study. The objective is to compare the efficacy of these inversion methods over F3 block seismic data. For post-stack inversion, the data was inverted into a very high-resolution P-impedance volume. The analysis depicts that all four inversion methods provide mutually consistent subsurface information with marginally better MBI results. Furthermore, geostatistical techniques have been used intensively for further testifying the results obtained from post-stack inversion methods. The geostatistical techniques use seismic data-derived attributes and inverted impedance-derived attributes as input to estimate P-wave velocity, porosity, and density away from the boreholes. Two geostatistical methods namely probabilistic neural network (PNN) and multilayer feed-forward neural network (MLFN) are used for the analysis. Porosity, density, and P-wave velocity have been predicted using both techniques which highlighted different characteristics of the subsurface with very detailed information. The derived results show that reservoir properties have been better estimated with the combination of MBI and PNN techniques for F3 block data over the other methods used in this study.

*Corresponding Author

Email: mauryasatya@bhu.ac.in
Tel: +(91) 982 085 1470

1. Introduction

In contrast to well-log data, which can provide comprehensive layer information but is typically quite sparse, seismic data contains amplitude with time and can only provide information on the subsurface interface. Seismic and well-log data need to be combined to provide precise information on the subsurface rocks and fluids in the inter-well region. The seismic inversion method combines well log and seismic data to get precise information about the subsurface. Seismic inversion is a method for converting low-resolution seismic reflection data into a high-resolution subsurface model of rock and fluid characteristics utilizing high-frequency well-log data. In the petroleum industry, seismic inversion techniques are widely used to characterize reservoirs using seismic data.

Reservoir characterization typically specifies the total volume inside the trap, which can contain hydrocarbons. The key elements in interpretation are the precision of reservoir approximation such as thickness as well as other petrophysical parameters of each reservoir, and reservoir properties estimation, such as water saturation, porosity, and other parameters from well log and seismic data. Seismic data can estimate reservoir parameters quantitatively throughout the analysis; one such fundamental step is to relate the seismic volume at the well position often via a synthetic seismogram (a sonic and density logs-derived seismic trace). Efforts throughout the study concentrate on predicting the physical sub-surface properties of rocks that are essential in the discovery and extraction of hydrocarbons. A significant element in quantifying producible hydrocarbons is the understanding of reservoir characterization [1-5]. It is possible to obtain precise reservoir characterization from well logs, mainly utilizing resistivity logs and gamma rays [2]. Supplementary studies of the geological structure that can keep hydrocarbons in place must be considered to map hydrocarbon reservoirs as hydrocarbons in geological traps, i.e., a rock formations combination that will prevent vertical or lateral migration of gas and oil. The progress of a diversity of methods that try to spread log properties has been motivated by the need to thoroughly analyze targets to identify ideal production approaches and also reduce the threat that may be correlated with the exploration of hydrocarbon [6-9].

In the present study, four types of seismic inversion namely, model-based inversion (MBI), colored inversion, bandlimited inversion, and maximum likelihood sparse spike inversion methods are used to estimate subsurface acoustic impedance. The MBI is a form of post-stack inversion that estimates acoustic impedance (P-impedance) from seismic data with inputs from well logs [10-13]. In this method, the error between synthetic and seismic data is minimized by updating the model and the least error model gives final results. On the other hand, the CI method is another post-stack inversion method in which the inversion is interpreted as a convolutional procedure where a frequency domain operator is utilized to convert the seismic traces into acoustic impedance [14, 15]. The bandlimited inversion methods use the relation between impedance and reflectivity for the inversion of seismic data. BLI method is the most common form of the inversion method, which presumes that the seismic amplitude is related to the coefficient of reflection and transforms the input seismic trace into P-impedance traces. The input seismic trace is normally wavelet processed [12]. Further, the MLSSI technique is the next inversion method applied here, but unlike other techniques, it provides a reflectivity series calculation that would estimate the seismic information with a minimum amount of (Sparse) spikes. In this scenario, non-uniqueness is expected to be taken care of by implementing the sparse criterion of reflectivity. To achieve this, the maximum likelihood deconvolution (MLD) was performed [10, 12].

Intelligent process is an efficient tool between two data sets to extract mathematical formulation. And in recent years it has continued to spread to the oil industry [16-21]. Both reservoir characteristics and seismic characteristics are essential [22-27]. Reducing the chance of finding productive sands and defining the boundaries of such sands are the two main issues we face in reservoir studies in clastic environments. The quality of data is also crucial to characterize the reservoir [28]. The latest approach to fixing such difficulties includes producing seismic attributes, which are physically associated with the reservoir properties, and merging these attributes to estimate the petrophysical properties of the reservoir [28-30]. Therefore, it is possible to predict porosity as well as the density of the reservoir by using seismic data and attributes. Previous research has already shown that reservoir porosity and density can be measured using statistical methods and intelligent systems [10, 31-33]. However, the majority of the time, neural network techniques rely on a linear fit between seismic features and

reservoir properties [34-37]. This paper aims to use seismic attributes to estimate petrophysical parameters from well-log data by applying PNN and MLFN neural network techniques.

The aim is to deliver a mechanism that will permit us to recognize and estimate the behavior of the reservoir and lessen the ambiguity. Geophysicists constantly struggle to categorize heterogeneities in the reservoir because seismic-guided prediction of petrophysical characteristics differs from those estimated in the borehole. The neural network techniques can aid in the resolution of this issue by supplying volumes of predicted reservoir parameters and ambiguities in such volumes. Then these volumes can be used to characterize the 3-D extent of the relevant sand facies.

The ability to create a nonlinear link between seismic qualities and well-log properties is the PNN's strength. The other neural network techniques are the multi-attribute regression method, MLFN, and radial basis function (RBF) method. The probabilistic neural network (PNN) is a modern nonlinear neural network model created on the statistical hypothesis [38-40].

Prediction of petrophysical parameters has been made by use of PNN and MLFN. The basic principle behind these techniques is to find a connection between attributes and petrophysical parameters. These relations were then used to interpolate or extend the properties to the entire seismic volume with some external attributes like impedance as constraints. These techniques help interpret the fluid content, lithology, saturation, and limits of the subsurface strata and productive zones [41-43]. Porosity, density, and P-wave volumes have evolved from geostatistical methods with inputs from seismic and well-log data as internal attributes and inverted impedance from MBI, CI, MLSSI, and BLI methods as external attributes. MBI, CI, MLSSI, and BLI methods were applied to the F3 block, Netherland seismic volume. The geostatistical techniques (PNN and MLFN) have been religiously applied to estimate various petrophysical parameters and to compare the various geostatistical techniques in predicting the parameters.

2. Study Area

The data sets used in this analysis contain four wells and post-stack 3D seismic data from F3 Block, Netherlands. Exploring the oil and gas reserves in the Upper-Jurassic to Lower Cretaceous layer, which is often located below the stated interval, was the goal of this survey. Reflectors from the Miocene, Pliocene, and Pleistocene make up the upper part up to 1200ms [15, 44, 45]. With a very high porosity, sand and shale make up the deltaic bundle (20-42%).

Within the survey region, there are four vertical wells, and each well has sonic and gamma-ray logs. The well log's depth was roughly 1700ms [45]. The seismic survey region comprises from cross-line 300 to 1200 and inline 100 to 750. The locations of wells F02-1, F03-2, F03-4, and F06-1 are 362 inline and 336 cross line, 722 inline and 848 cross line, 442 inline and 1007 cross line, and 244 inline and 387 cross line, respectively. dGB Earth Sciences (An open-source seismic repository portal) offers both seismic and well data used in this study. Fig. (**1**) represents the location map of the study area, along with the survey region and location of wells. Within the survey region, there are four vertical wells, and each well had sonic and gamma-ray records with a depth of around 1700ms. The placement of the wells is at 362 inline and 336 crossline for F02-1, 722 inline and 848 crossline for F03-2, and 244 inline and 387 crossline for F03-4. The seismic survey region covers the crossline and inline distances of 300 to 1200. P-wave sonic, density, S-wave sonic, and check shot logs are the crucial pieces of information required for the inversion process.

3. Methodology

The research methodology is described step-wise in the following sections. However, it is appropriate to mention at this stage that due to the paucity of well and seismic log data from Indian oil fields and the regulatory bodies, the study was performed on open-access data provided by F-3 Block, Netherlands. The main impetus for formulating the methodology, after obtaining the data, was on obtaining the seismic-well log tie, performing a host of prevalent inversion techniques, and finally verifying the inversion-based results by rigorously using the

state-of-the-art geotechnical techniques to gather the pertinent parameters to delineate the reservoir. The reservoir characterization is largely done by post-stack methods, but by using various geostatistical techniques for characterizing the geophysical parameters is the way forward, which makes the characterization of the reservoir much [18-24]. Therefore, rigorous scrutiny and implementation of various post-stack data in conjunction with the use of recent geostatistical techniques has brought forth the novelty component in the present research and has made the research findings very trustworthy.

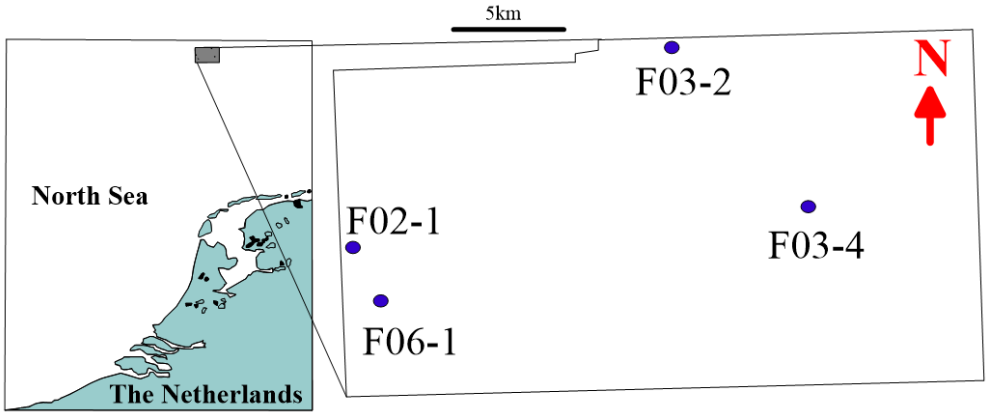

Figure 1: The location map of the F3 block, Netherlands (After Kushwaha *et al*., 2020).

3.1. Seismic Inversion

In the current research, post-stack inversion techniques are used for the characterization of reservoirs. For this, seismic and well-log data are used as input providers. The research has used the CGG Veritas Hampson Russell Software (HRS) package to estimate the volume of P-impedance from various post-stack inversion methods over the F3 block, Netherlands.

The first seismic inversion method used in this study is the model-based inversion method which is very common nowadays. In this method, an acoustic impedance model is created based on a prior study, and a synthetic section is generated using a forward modeling technique. For the forward modeling, the following equation can be used.

$$S(t) = W(t) * R(t) + N(t) \quad (1)$$

Where S(t) is a synthetic trace, W(t) is a ricker wavelet, R(t) is reflectivity assumed based on prior information and N(t) is the noise component. Once the synthetic data is generated, the least square error is estimated between synthetic and real data and the least square optimization is used to minimize error. The error is minimized by updating reflectivity R(t) and the least error model is assumed real subsurface model which is the desired output of model-based inversion methods. The second seismic inversion method used in this study is colored inversion.

In a seismic colored inversion, first, the spectrum of the operator is computed using the spectra of the acoustic impedance obtained from log data. Since this operator's phase is -90°, it can be integrated with the reflectivity series to produce impedances. The operator can be designed using seismic and well-log data. For all of the nearby wells, the acoustic impedance is first estimated and displayed against frequency. To express the impedance spectrum in the subsurface in the log-log scale, a regression line is fitted to the amplitude spectrum of the acoustic impedance. Second, using seismic traces close to the wells, the seismic spectrum is determined. The operator spectrum, which converts the seismic spectrum into the average impedance spectrum, is calculated using these two spectra. Third, to construct the necessary operator in the time domain, the final spectrum is mixed with a -90° phase shift. The third seismic inversion method used here is the bandlimited inversion method which is the oldest technique and is still in use and provides good results.

Seismic bandlimited inversion uses the relationship between impedance and reflectivity and the derived relation between impedance and seismic trace. The desired relation can be written as follows:

$$Z_{j+1} = Z_1 \exp\left(\gamma \sum_{i=1}^{j} S_i\right) \quad (2)$$

The last seismic inversion used in this study is maximum likelihood sparse spike inversion (MLSSI) which is based on the l_2 norm. In this method, a sparse reflectivity sequence is computed for each trace by adding reflection coefficients one at a time until the best set is identified. The broadband reflectivity is then gradually changed until the synthetic trace produced is within a certain tolerance of the genuine trace. How far the algorithm deviates from the initial guess model to match the actual data can be managed. Apart from these four seismic inversion methods, two types of geostatistical methods are used to predict various petrophysical parameters.

3.2. Geostatistical Techniques

The state-of-the-art geostatistical tools have been used to further estimate various petrophysical parameters like density, porosity, and P-wave velocity for F3 block post-stack seismic data. The P-impedance derived from MBI methods has been used as an external attribute while attributes extracted directly from seismic data (seismic attributes) were used as internal attributes in the geo-statistical investigation.

The geostatistical techniques use seismic data-derived attributes and inverted impedance-derived attributes as input to estimate various petrophysical parameters far from the boreholes. The four categories of these geostatistical techniques are single-attribute analysis, multi-attribute regression, PNN, and MLFN. PNN and MLFN derive nonlinear relationships rather than linear relationships as in a single attribute and multi-attribute case [10, 23-35].

Two types of geostatistical techniques, i.e., PNN, and MLFN have been used for the prediction of petrophysical properties. The training time of the PNN method is shorter and accuracy is better than the traditional multilayer forward network (MLFN) method. It is specifically beneficial for the nonlinear multi-attribute regression method. PNN has outstanding performance on unseen data.

PNN is a subset of radial basis function networks and conditional Bayes statistical methods. PNN's mechanism matches human behavior [46-49]. Another form of neural network is the PNN [11-13, 50]. It depends on the estimation of the probabilistic density function of Parzen. PNN is a feedforward neural network with a complex structure. It comprises an input layer, a pattern layer, a layer of summation, and an output layer [41]. PNN is, in actuality, a form of computational interpolation, but it has a neural network structure. It has a more significant function of interpolation than MLFN.

The PNN method consists of one input layer, one or more hidden layers, and one output layer that makes up the MLFN network. Each network layer comprises of nodes which are linked to each other. Their connections are termed as weights. These weights are the concluding component of the output decision as they play a very significant role in the execution of MLFN. The required number of attributes to be examined during the MLFN process determines the number of input nodes. The basic architecture of MLFN is shown in Fig. (**2**). This is the difference between PNN and MLFN methods.

4. Software Used for Data Analysis

The geophysical application software package Hampson-Russell (a subsidiary of CGG Veritas) has been used to execute the research in this study. Geoview was a well-database application for viewing logs. All post-stack seismic inversion procedures were accessible in various modules of the Hampson- Russell Software (HRS) and the same has been used for processing and interpreting the data. EMERGE was a tool of HRS for performing geostatistical analysis.

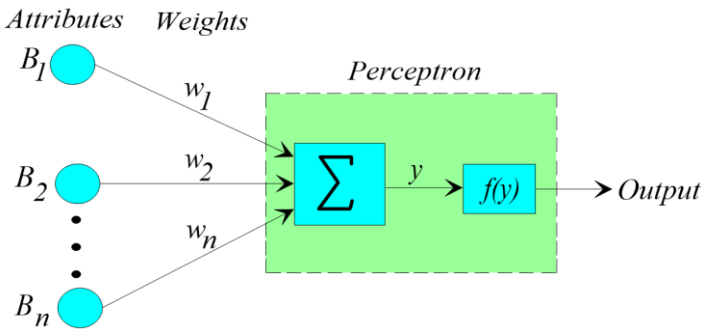

Figure 2: The architecture of the MLFN technique.

5. Results and Discussion

5.1. Application of Seismic Inversion

The seismic inversion is performed in this study using the following steps.

5.1.1. Seismic Data

In this study, post-stack seismic data have been used. Representative post-stack data from the F3 block, the Netherlands are shown in Fig. (**3**). This seismic data is used as input in all types of seismic inversion methods.

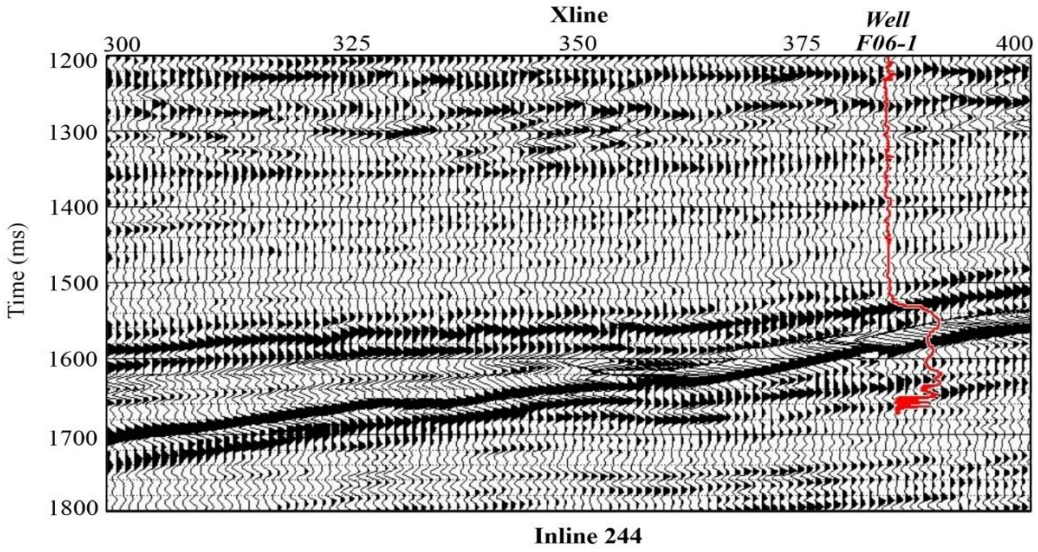

Figure 3: A representative post-stack data from F3 block, the Netherlands.

5.1.2. Well Log Data

Well-log data is used as an input with seismic data which shows the variation of petrophysical properties with depth. There are four wells F02-1, F03-2, F03-4, and F06-1 are used in the analysis and one well (F02-1) is displayed in Fig. (**4**).

5.1.3. Horizon Picking

A theoretical layer of earth is generally known as a demonstration of sedimentary surfaces and the boundary between two sedimentary layers is known as horizons [51]. These horizons reveal contact characteristics between two rock bodies containing dissimilar porosity, fluid content, density, seismic velocity, etc. in the seismic section. The application of seismic data interpretation is performed based on these horizons. These horizons are crucial to

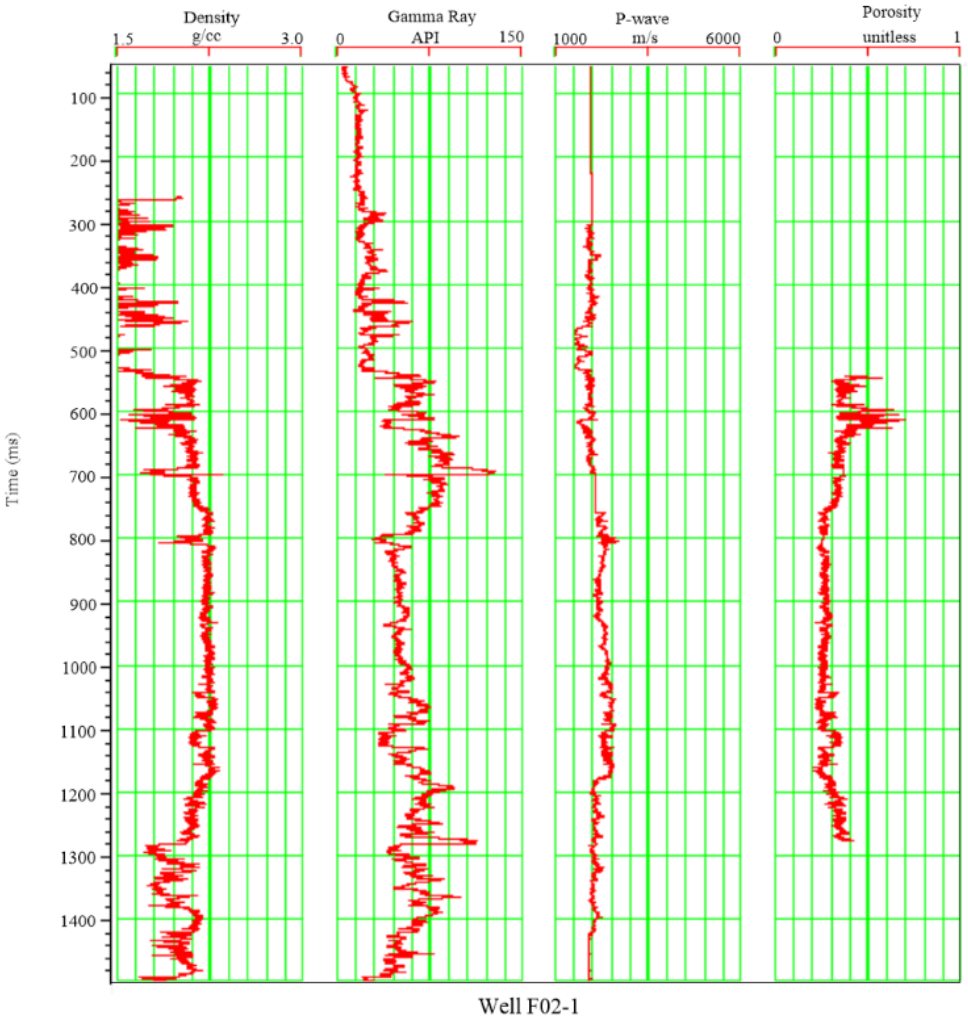

Figure 4: A representative well log plot from F3 block, Netherlands.

seismic inversion techniques because they serve as a reference for interpolating well log characteristics between wells. Picking the seismic horizon is a herculean job as it needs real technical expertise, understanding, time, and concentration. The red-colored division line represents a manually picked horizon in Fig. (**5**).

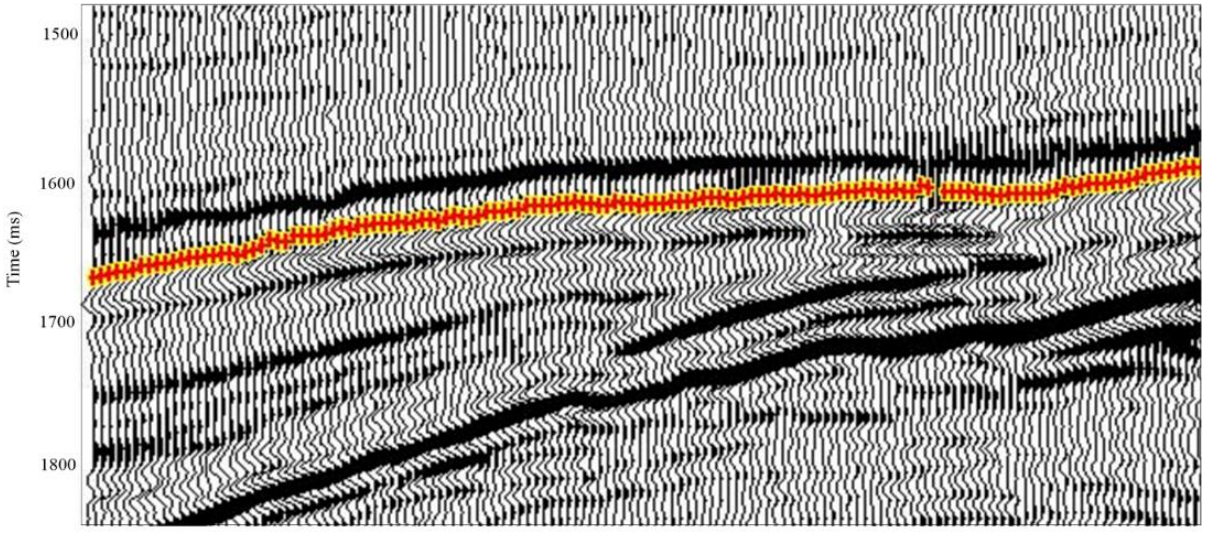

Figure 5: A representative image of horizon picking (from HRS).

5.1.4. Wavelet Estimation

In most of the inversion methods, the seismic wavelet is used to generate synthetic data which is further utilized to estimate error between synthetic and seismic data followed by the application of optimization to reduce error hence the wavelet estimation becomes a very crucial step. The process of wavelet extractions is as follows:

1. To extract and taper the seismic traces.
2. To compute the autocorrelation based on the length of the preferred wavelet.
3. To compute the autocorrelation frequency spectrum.
4. To obtain the square root of the frequency spectrum modulus by silencing the zero hertz component.
5. To compute the inverse FFT. The original component of the inverse FFT output is the zero-phase wavelet [52].

A seismic wavelet is the source signature of the seismic data and the relation between the geology (reflection coefficients) and the seismic data (traces). Without knowing the wavelet, several valid interpretations of the subsurface cannot be made [52]. Therefore, wavelet extraction is perhaps the most important step in the seismic well tie, which is the correlation of a synthetic seismogram computed from well log data with the help of seismic data. The synthetic seismogram is the convolution results between a wavelet and reflectivity derived from well logs. Fig. (**6**) reveals the extracted zero-phase Ricker wavelet.

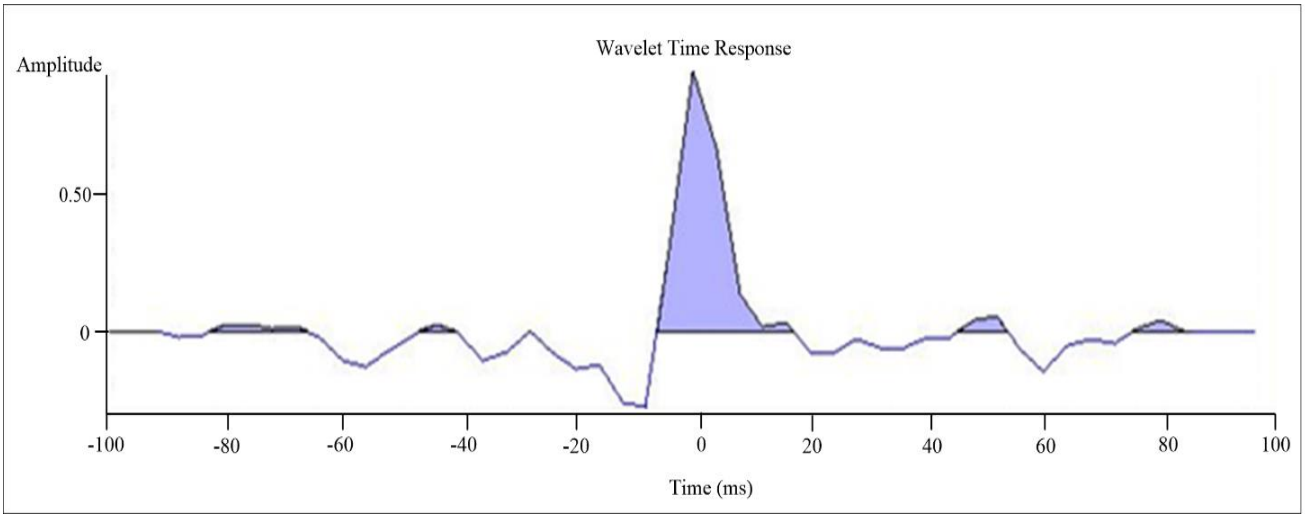

Figure 6: Statistical zero-phase seismic wavelet.

5.1.5. Seismic to Well Tie

Correction of the log data and seismic sections is finished using the check shot log. A check shot is a log that is capable of transforming other geophysical logs from depth to time domain, that correlate seismic and well log data. Integrating and calibrate information from well log data with the seismic is the objective of seismic to well tie. The seismic to-well tie can also be performed using a manual created and plotted side by side with seismic traces. The procedure of manually matching the synthetic seismic waveform and reflection seismic waveform known as seismic to well tie is performed as follows. [10, 40].

- A synthetic trace was produced by utilizing well log data and comparing it with the nearest seismic trace at the well location.
- Time squeezing and stretching were then implemented to the data to match the well-log and seismic reflectors.

The correlation coefficient (CC) and residual error have been computed between the seismic traces and modified synthetic traces from the well log. A representative Fig. (**7**) indicates the results of a seismic well tie. The seismic well tie and wavelet estimation were performed for all the wells within the seismic survey. Each well has an optimum wavelet obtained from the preceding seismic well tie loop. Usually, the optimum wavelets obtained for each well are unique. The final wavelets were obtained by averaging all the optimum wavelets. The blue traces show pseudo synthetic traces produced using well log and wavelet. The red traces show seismic traces close to the well location. The black traces show real seismic gathers.

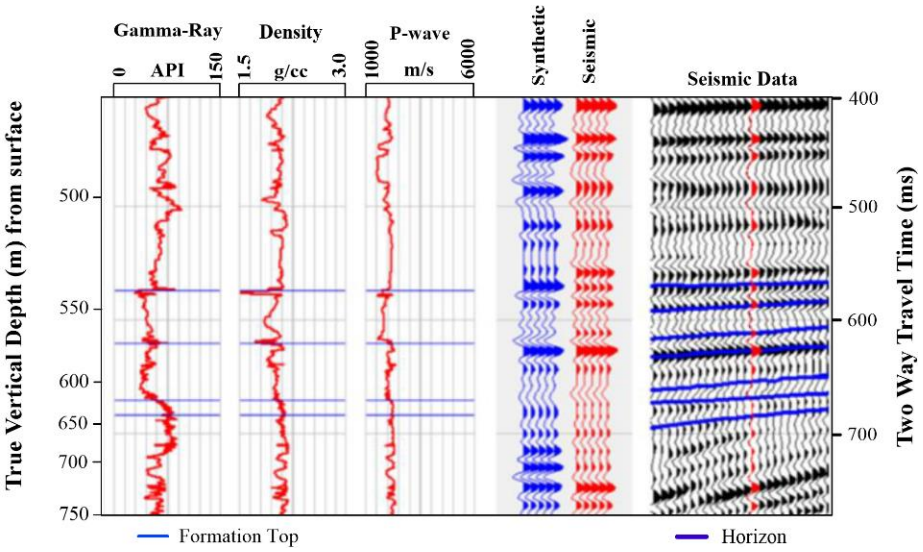

Figure 7: A representative seismic well tie using well log data with the help of seismic data.

5.1.6. Building Initial Model

In this step, preliminary petrophysical properties models are configured. These preliminary models have been constructed by interpolating the petrophysical properties from well positions into the seismic section along the crosslines and inlines. As a guide for the interpolation interpreted seismic horizons are used. In a post-stack inversion, a P-impedance model is constructed which is a letter used for the seismic inversion process.

5.1.7. Inversion Analysis at Well Locations

In this step, post-stack inversion methods are performed to estimate petrophysical properties. To cross-check the inversion algorithm, the composite trace close to the well location is used. This is performed for all the wells available in the study area. If found satisfactory, then this analysis could be used to predict volumes of petrophysical properties. If satisfactory results are gathered then, the algorithm would be performed for the whole volume. For this, the inverted P-impedance volume is derived from all post-stack inversion methods. The interpretation of the entire study area depends upon these inverted results.

The post-stack inversion has been done on the F3 block, in the Netherlands. All four inversion methods (MBI, CI, MLSSI, and BLI) have been found to provide similar trends but at different confidence levels, based on the degree of correlation and residual average error values. These methods have been closely scrutinized at the well locations to compare the inverted results of the P-impedance with the log impedance. The inversion analysis has been performed for all the wells but only well F06-1 results are presented for simplicity. The correlation of well F06-1 for MBI, CI, MLSSI, and BLI is 0.99, 0.85, 0.89, and 0.87, respectively (Figs. **8**, **10**, **12** and **14**). From the inspection of inversion analysis results, it is discernible that MBI has yielded the best correlation results (0.99) while CI yielded the least correlation (0.85) among the four inversion methods. The cross plots for all the inversion methods between original and inverted impedance are also presented in Figs. (**9**, **11**,**13** and **15**), respectively. The distribution of points is near the best-fitted line, which indicates that the original and inverted impedances are close enough to each other. MBI cross plot shows a good best-fit line in comparison with the other three methods (Fig. **9**).

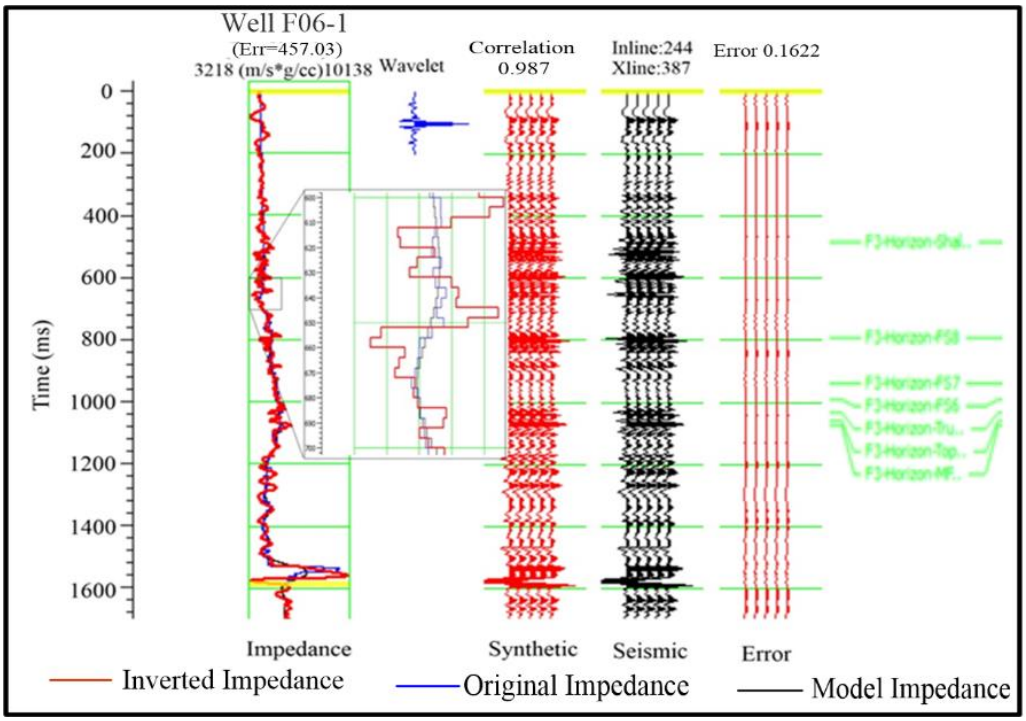

Figure 8: Inversion analysis result obtained from MBI method with correlation 0.99.

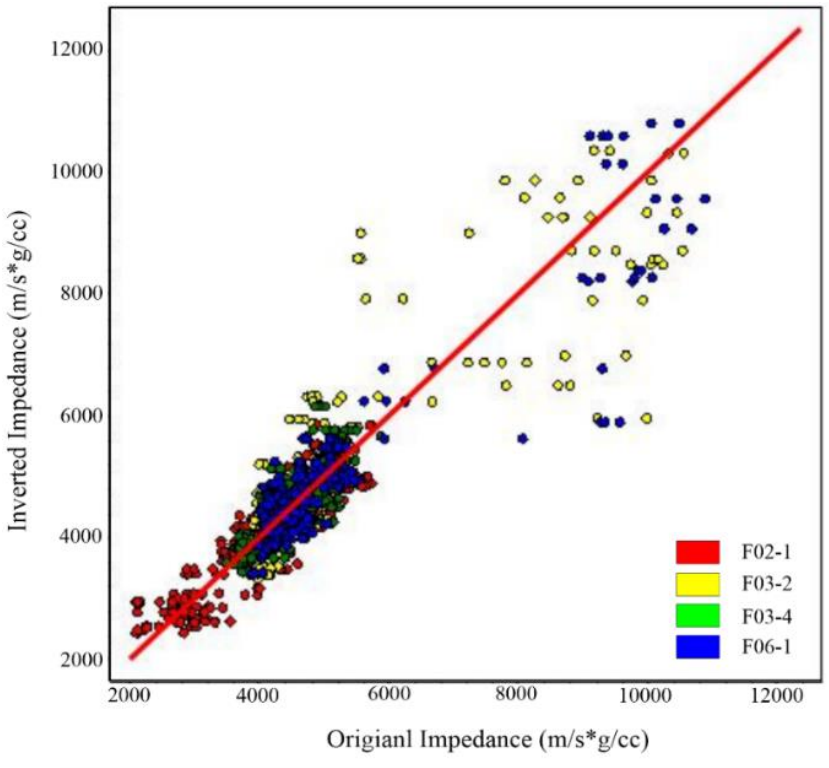

Figure 9: Cross plot between original impedance and inverted impedance obtained from MBI method.

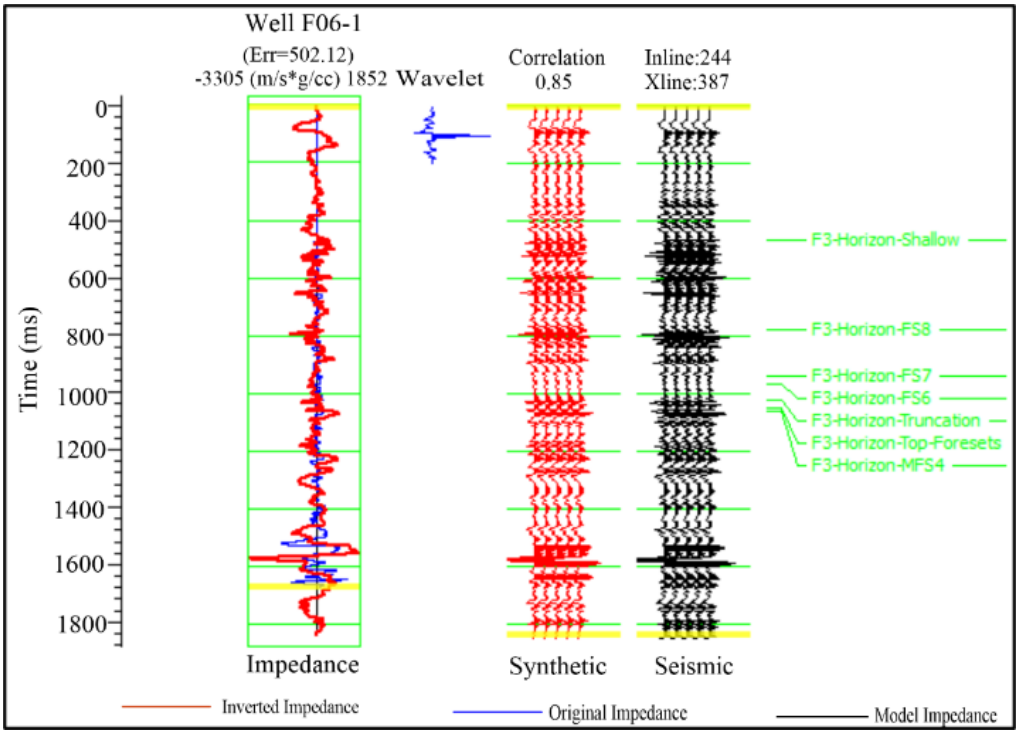

Figure 10: Inversion analysis result obtained from CI method with correlation 0.85.

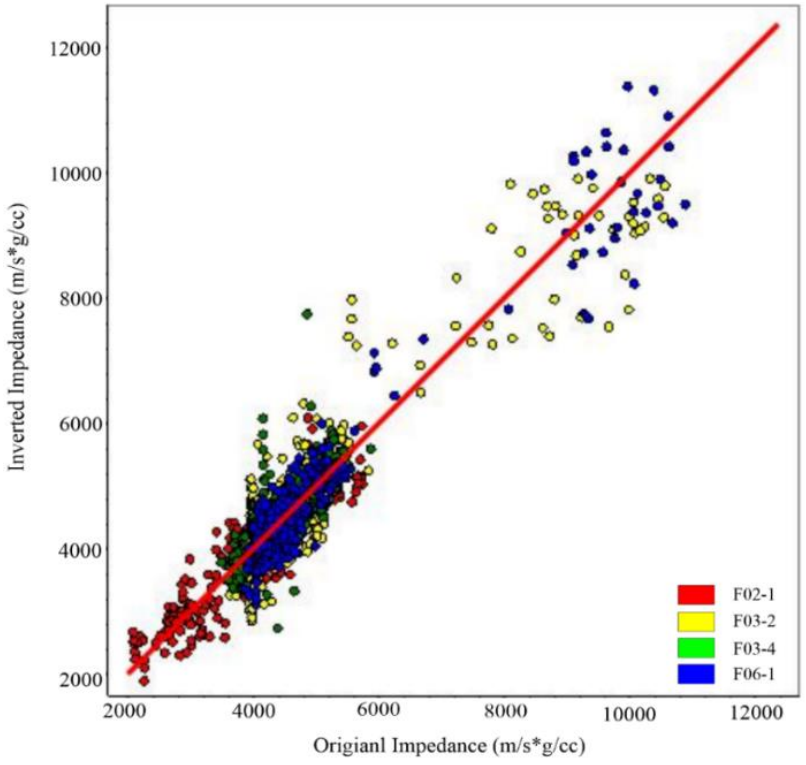

Figure 11: Cross plot between original impedance and inverted impedance obtained from CI method.

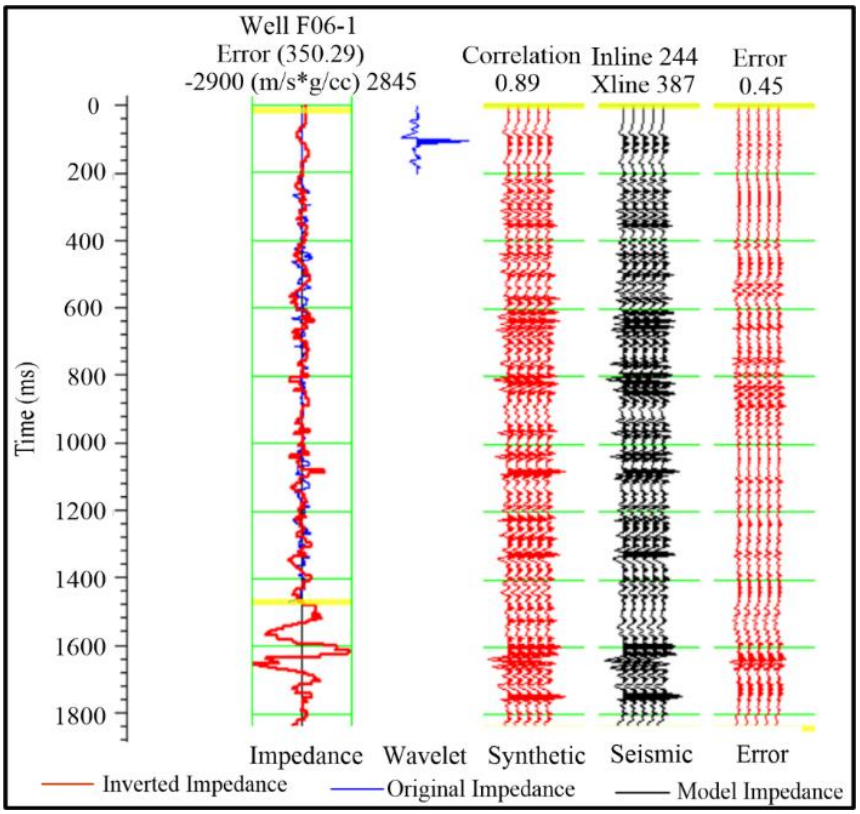

Figure 12: Inversion analysis result obtained from MLSSI method with correlation 0.89.

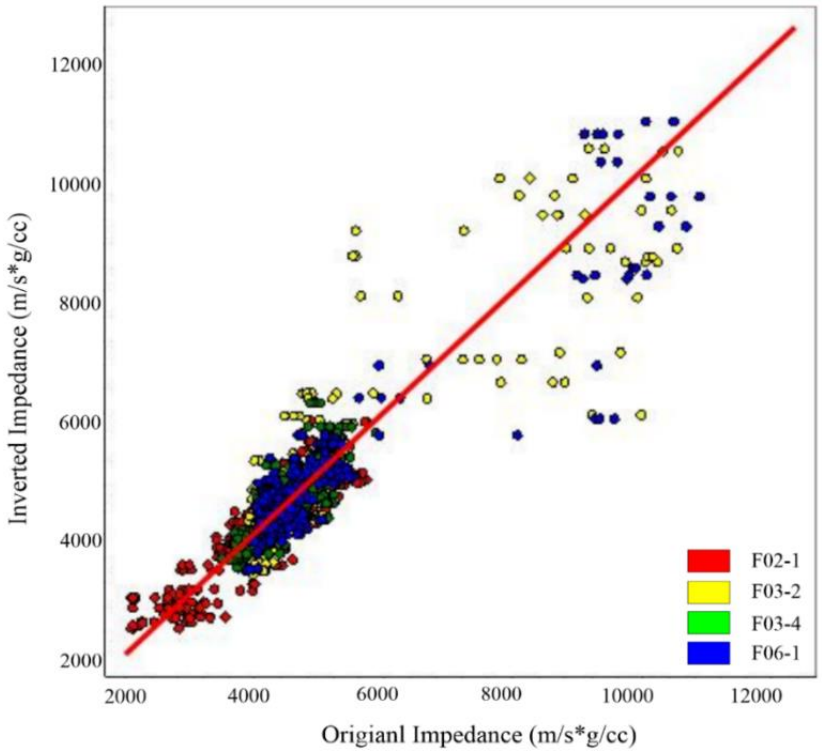

Figure 13: Cross plot between original impedance and inverted impedance obtained from MLSSI method.

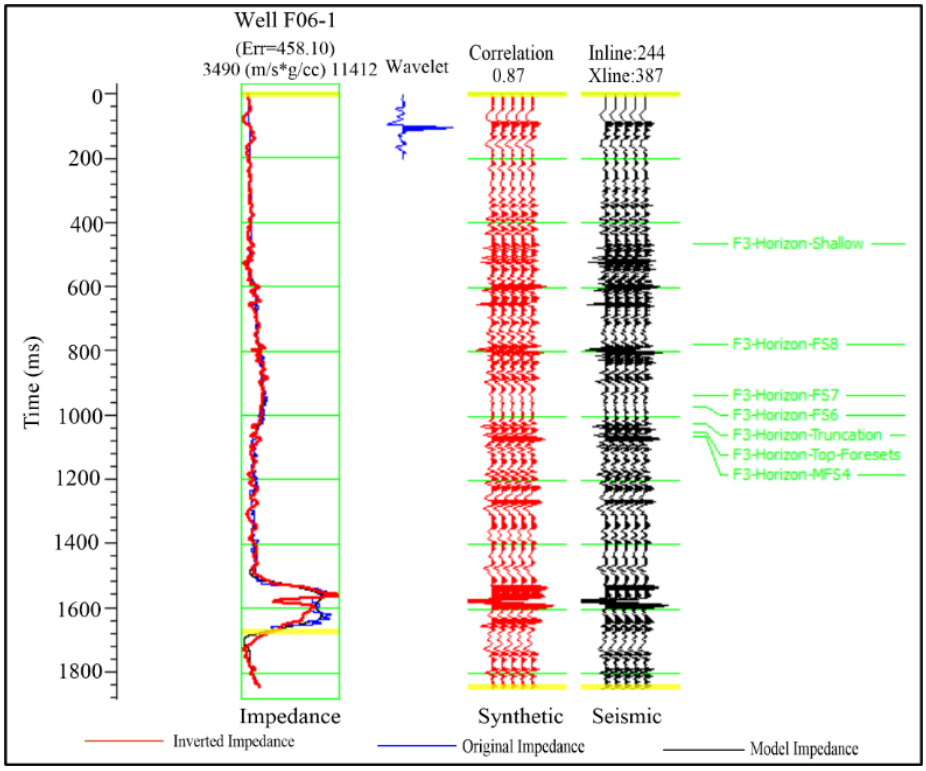

Figure 14: Inversion analysis result obtained from BLI method with correlation 0.87.

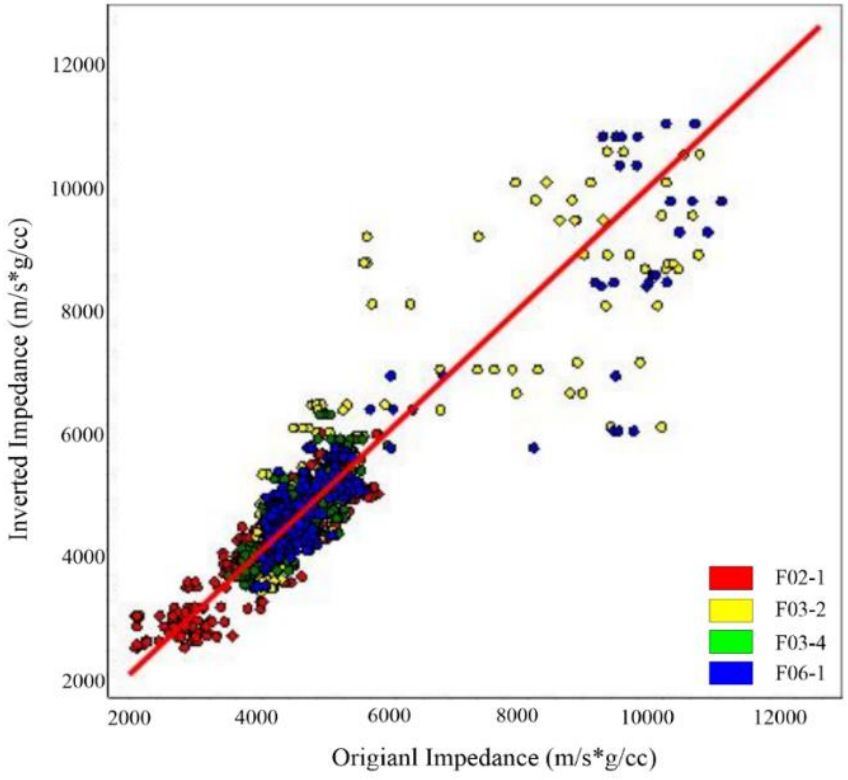

Figure 15: Cross plot between original impedance and inverted impedance obtained from BLI method.

5.1.8. Entire Seismic Volume Inversion

Thereafter, inversion of the entire seismic volume for all inversion methods have been performed, and impedance volumes estimated (Fig. **16**). Fig. (**16**) provides a visual overview of all the four post-stack inversion methods (Crossline 600-900, Inline 244). For convenience, inverted impedance cross-sections have been represented only between 1500ms to 1850ms time intervals, which is described as an anomalous zone. The low P-impedance region has been highlighted by the arrows in the figures for each inversion method. This reveals that MBI provides better amplitude correlation, lower average impedance values, and the best vertical resolution, and detects the geological inconsistencies in the horizontal layers than the other three inversion methods. The reason behind the accuracy of MBI performance may be attributed to the fact that iteratively changing the acoustic impedance model is done until the difference between the seismic trace and the inverted trace is below a certain point.

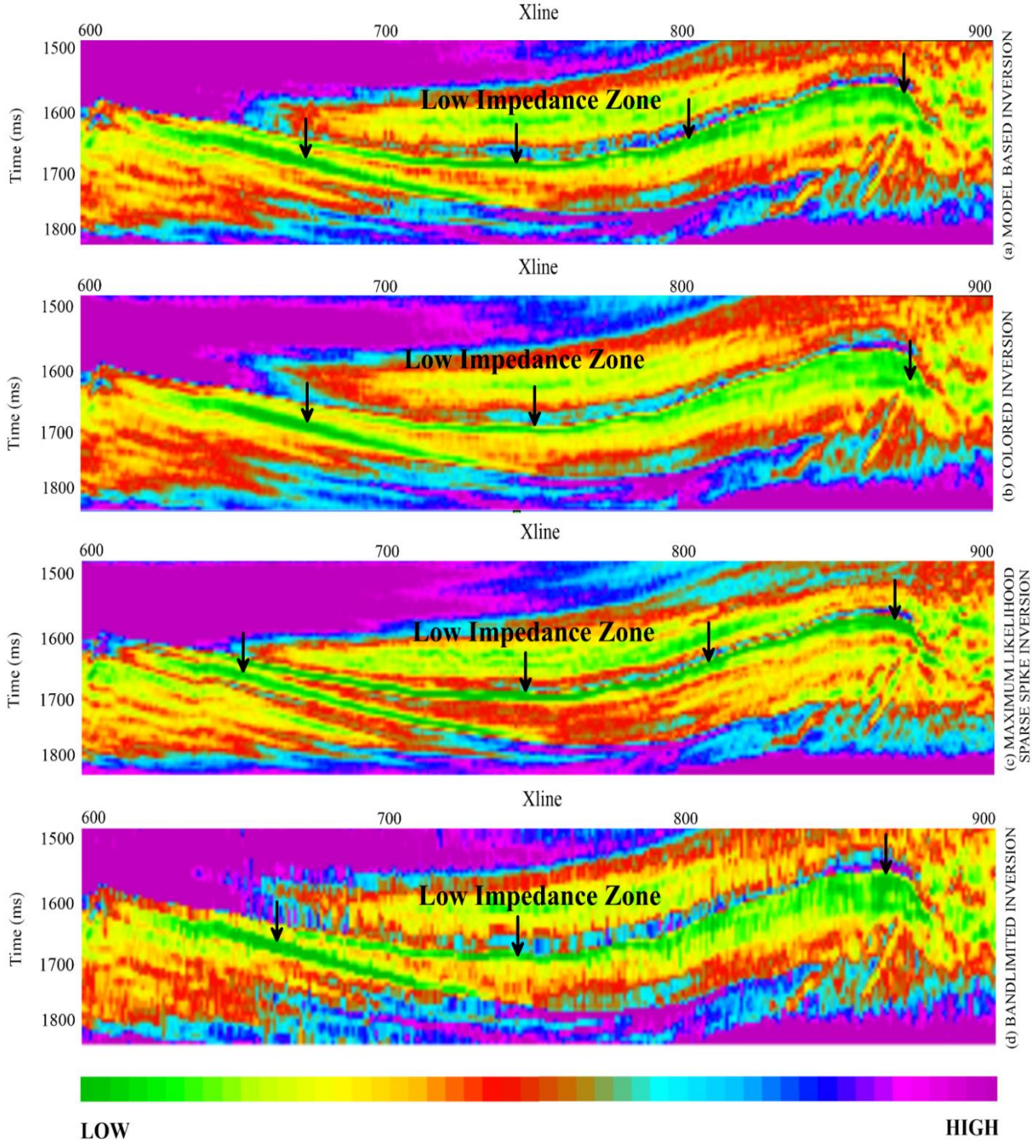

Figure 16: Estimated acoustic impedance using (a) MBI, (b) CI, (c) MLSSI, and (d) BLI methods.

5.2. Application of Geostatistical Methods

For geostatistical analysis, two different methods namely probabilistic neural network (PNN) and multilayer feed-forward neural network (MLFN) techniques are used for different petrophysical parameter prediction. These geostatistical methods use inverted impedance as input and hence the best results estimated by MBI are utilized for this purpose. PNN and MLFN-generated predicted volumes are illustrated in Figs. (**17**) and (**18**), respectively.

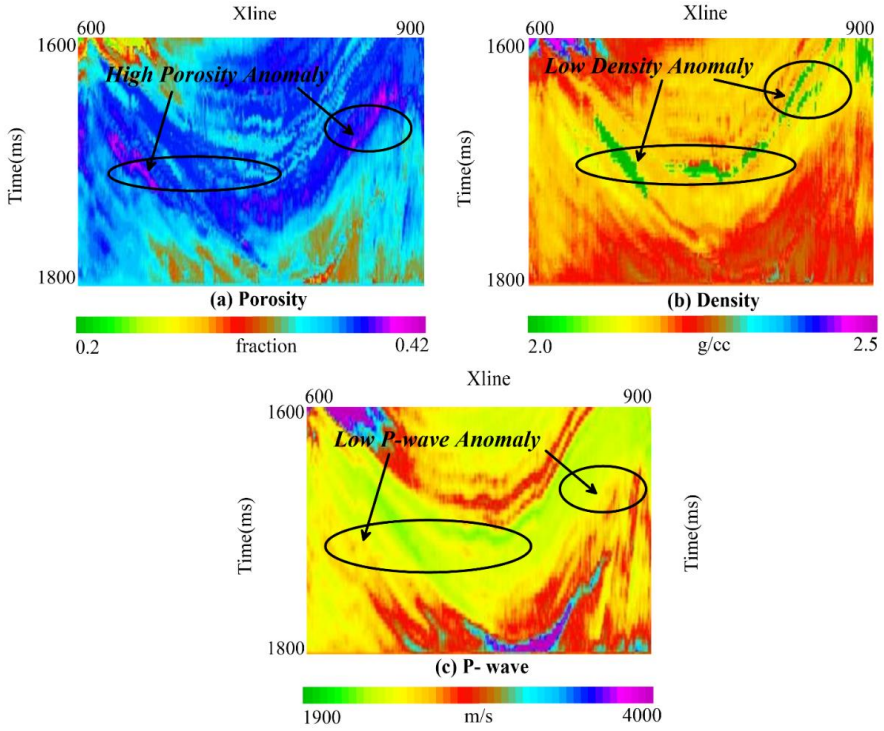

Figure 17: Predicted volumes using PNN for (a) porosity, (b) density, (c) P-wave (Inline 244).

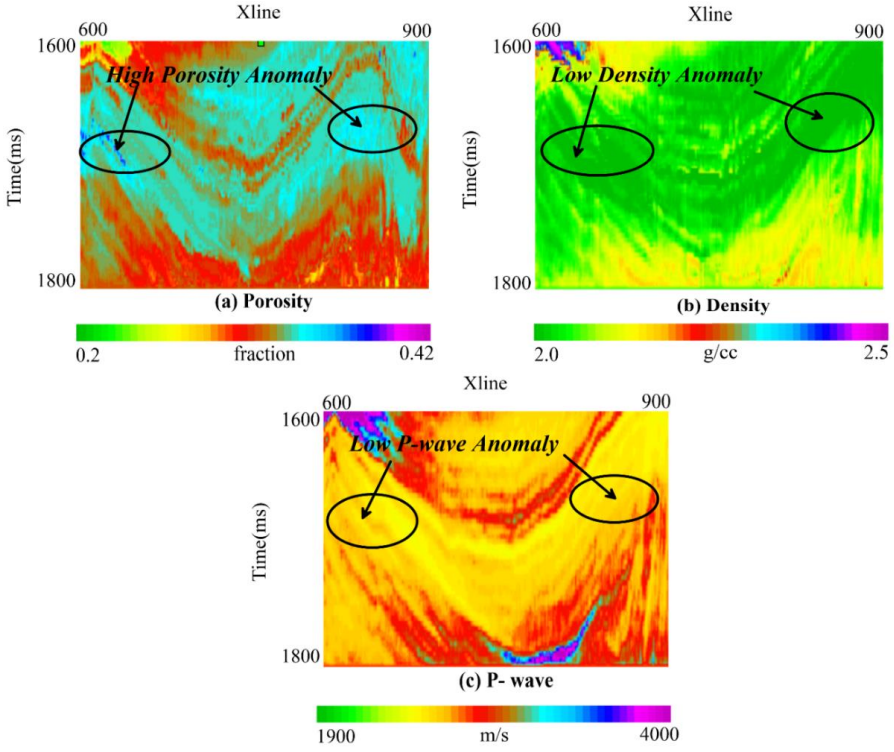

Figure 18: Predicted volumes using MLFN (a) porosity, (b) density, (c) P-wave (Inline 244).

The anomalous zones are also highlighted by an ellipse in Fig. (**17**) and (**18**). The predicted volumes from the PNN algorithm gave a slightly better resolution than MLFN predicted volumes. This geostatistical estimated section is more revealing as compared to the seismic data due to two reasons; firstly, the section is giving layer property whereas the seismic data is supplying interface property and secondly, it interpolates the well log property into the seismic sections to offer thorough information. The 1700ms time interval is determined to be an anomalous zone.

6. Conclusion

In the present study, four types of seismic inversion namely model-based inversion (MBI), colored inversion (CI), bandlimited inversion (BLI), and maximum likelihood sparse spike inversion (MLSSI) is utilized for the inversion of seismic data. The results show that although MBI, CI, MLSSI, and BLI methods have provided good results by distinctly demarcating the low-impedance zone corresponding to the target reservoir, the MBI method has yielded the best results. These inversions estimated subsurface acoustic impedance from post-stack seismic data which provided very high-resolution subsurface information and helps to interpret different rock and fluid properties. The study also demonstrated two very powerful geostatistical methods namely probabilistic neural network (PNN) and multilayer feed-forward neural network (MLFN). These geostatistical methods are used to predict porosity, density, and P-wave velocity in the inter-well region. The low impedance, high porosity, low density, and low P-wave velocity, volumes derived from post-stack and geostatistical techniques suggest the presence of an anomalous zone between 1680ms to 1700ms time interval. This time interval zone is equivalent to 1680m of the depth of occurrence of the reservoir from the ground surface. The outcomes suggest that PNN is a trustworthy method of porosity and density estimations among the methods applied in this study.

Acknowledgments

We thank GeoSoftware for providing Hampson Russell software, particularly Emerge and Geoview. In addition, we acknowledge the academic licenses for Matlab (2022b) and Norsar (full package), respectively, from www.mathworks.com and www.norsar.no respectively. This work couldn't be done without their help.

Conflict of Interest

The authors declare that there is no conflict of interest.

Funding

Dr. Satya P. Maurya, expresses gratitude to the funding organizations UGC-BSR (M-14-0585) and IoE BHU (Dev. Scheme no. 6031B) for their financial assistance.

References

[1] Schlumberger. Log interpretation, principle, and application: schlumberger wireline and testing. Int J Geosci 1989; 7: 21-89.

[2] Asquith N. Basic well log analysis for geologists. Tulsa: A.A.P.G. Methods in Exploration; 1982. https://doi.org/10.1306/mth3425

[3] Aminu MB, Olorunniwo MA. Reservoir characterization and paleo-stratigraphic imaging over Okari Field, Niger Delta, using neural networks. Tulsa, OK: Leading Edge; 2011; 2: 650-5. https://doi.org/10.1190/1.3599150

[4] Tahmasebi P, Hezarkhani A. A fast and independent architecture of artificial neural network for permeability prediction. J Pet Sci Eng. 2012; 86: 118-26. https://doi.org/10.1016/j.petrol.2012.03.019

[5] Karimpouli S, Fathianpour N, Roohi J. A new approach to improve neural networks' algorithm in permeability prediction of petroleum reservoirs using supervised committee machine neural network (SCMNN). J Pet Sci Eng. 2010; 73: 227-32. https://doi.org/10.1016/j.petrol.2010.07.003

[6] Pendrel J. Seismic inversion- the best tool for reservoir characterization. CSEG Recorder. 2001; 26: 18-24.

[7] Chithra Chakra N, Song K-Y, Gupta MM, Saraf DN. An innovative neural forecast of cumulative oil production from a petroleum reservoir employing higher-order neural networks (HONNs). J Pet Sci Eng. 2013; 106: 18-33. https://doi.org/10.1016/j.petrol.2013.03.004

[8] Asoodeh M, Bagheripour P. ACE stimulated neural network for shear wave velocity determination from well logs. J Appl Geophy. 2014; 107: 102–7. https://doi.org/10.1016/j.jappgeo.2014.05.014

[9] Hampson D, Russell E. Maximum-likelihood seismic inversion (abstract no. SP-16). National 30 Canadian SEG Meeting, Calgary: 1985.

[10] Doyen PM. Porosity from seismic data: A geostatistical approach. Geophysics. 1988; 53: 1263-75. https://doi.org/10.1190/1.1442404

[11] Lancaster S, Whitcombe D. Fast-track coloured inversion. SEG Technical Program Expanded Abstracts 2000; 19: 1572-5. https://doi.org/10.1190/1.1815711

[12] Kushwaha P, Maurya S, Rai P, Singh N. Porosity prediction from offshore seismic data 10 of F3 Block, the Netherlands using multi-layer feed-forward neural network. Curr Sci. 2020; 119: 1652–62.

[13] Lindseth RO. Synthetic sonic logs—a process for stratigraphic interpretation. Geophysics. 1979; 44: 3-26. https://doi.org/10.1190/1.1440922

[14] De Bruin G, Bouanga E. Time attributes of stratigraphic surfaces, analyzed in the structural and Wheeler transformed domain. 69th EAGE Conference and Exhibition incorporating SPE EUROPEC, European Association of Geoscientists & Engineers; 2007.

[15] Wolak J, Hemstra N, Ochoa J, Pelissier M. Reconstruction of depocenter evolution through time using relative stratigraphic thickness. The Leading Edge. 2013; 32: 172-7. https://doi.org/10.1190/tle32020172.1

[16] Jain CK, Yerramilli SS, Yerramilli RC. A case study on blowout and its control in Krishna-Godavari (KG) basin, East Coast of India: safety and environmental perspective. J Environ Earth Sci. 2012; 2: 49-60.

[17] Kormylo JJ, Mendel JM. Maximum-likelihood seismic deconvolution. IEEE Transactions on Geoscience and Remote Sensing 1982; 1: 7-82. https://doi.org/10.1109/TGRS.1983.350532

[18] Bosch M, Mukerji T, Gonzalez EF. Seismic inversion for reservoir properties combining statistical rock physics and geostatistics: A review. Geophysics. 2010; 75: 75A165-76. https://doi.org/10.1190/1.3478209

[19] Chambers RL, Yarus JM. Quantitative use of seismic attributes for reservoir characterization. CSEG Recorder 2002; 27: 14-25.

[20] Chi C, Mendel JM, Hampson D. A computationally fast approach to maximum-likelihood deconvolution. Geophysics. 1984; 49: 550-65. https://doi.org/10.1190/1.1441690

[21] Krebs JR, Anderson JE, Hinkley D, Neelamani R, Lee S, Baumstein A, *et al*. Fast full-wavefield seismic inversion using encoded sources. Geophysics. 2009; 74: WCC177-88. https://doi.org/10.1190/1.3230502

[22] Russell BH. Introduction to seismic inversion methods. vol. 2. Tulsa: Society of Exploration Geophysicists; 1988. https://doi.org/10.1190/1.9781560802303

[23] Vecken PCH, Da Silva M. Seismic inversion methods and some of their constraints. First Break 2004; 22: 1-24. https://doi.org/10.3997/1365-2397.2004011

[24] Li Q. LP sparse spike impedance inversion. CGG Veritas: Hampson-Russell Software Services Ltd, CSEG; 2001.

[25] Leiphart DJ, Hart BS. Comparison of linear regression and a probabilistic neural network to predict porosity from 3-D seismic attributes in Lower Brushy Canyon channeled sandstones, southeast New Mexico. Geophysics. 2001; 66: 1349-58. https://doi.org/10.1190/1.1487080

[26] Eskandari H, Rezaee MR, Mohammadnia M. Application of multiple regression and artificial neural network techniques to predict shear wave velocity from wireline log data for a carbonate reservoir South-West Iran. CSEG Recorder. 2004; 29(7): 42–8.

[27] Maurya SP, Singh KH, Singh NP. Qualitative and quantitative comparison of geostatistical techniques of porosity prediction from the seismic and logging data. Marine Geophys Res. 2019; 40: 1-21. https://doi.org/10.1007/s11001-018-9355-6

[28] Kushwaha PK, Maurya SP, Rai P, Singh NP. Estimation of subsurface rock properties from seismic inversion and geo-statistical methods over F3-block, Netherland. Explor Geophys. 2021; 52: 258-72. https://doi.org/10.1080/08123985.2020.1815528

[29] Hampson DP, Schuelke JS, Quirein JA. Use of multiattribute transforms to predict log properties from seismic data. Geophysics. 2001; 66: 220-36. https://doi.org/10.1190/1.1444899

[30] Iturrarán-Viveros U. Smooth regression to estimate effective porosity using seismic attributes. J Appl Geophy. 2012; 76: 1-12. https://doi.org/10.1016/j.jappgeo.2011.10.012

[31] Leite EP, Vidal AC. 3D porosity prediction from seismic inversion and neural networks. Comput Geosci. 2011; 37: 1174-80. https://doi.org/10.1016/j.cageo.2010.08.001

[32] Na'imi SR, Shadizadeh SR, Riahi MA, Mirzakhanian M. Estimation of reservoir porosity and water saturation based on seismic attributes using support vector regression approach. J Appl Geophy. 2014; 107: 93-101. https://doi.org/10.1016/j.jappgeo.2014.05.011

[33] Masters T. Signal and image processing with neural networks: a C++ sourcebook. New York: John Wiley & Sons, Inc; 1994.

[34] Masters T. Advanced algorithms for neural networks: a C++ sourcebook. 1st edition. John Wiley & Sons, Inc; 1994.

[35] Kushwaha P, Maurya S, Rai P, Singh N. Prediction of petrophysical parameters using probabilistic neural network technique, Elsevier; 2021, p. 273–92.

[36] Kushwaha PK, Maurya SP, Singh NP, Rai P. Use of maximum likelihood sparse spike inversion and probabilistic neural network for reservoir characterization: a study from F-3 block, the Netherlands. J Pet Explor Prod Technol. 2020; 10: 829-45. https://doi.org/10.1007/s13202-019-00805-3

[37] Miguez R, Georgiopoulos M, Kaylani A. G-PNN: A genetically engineered probabilistic neural network. Nonlinear Anal Theory Methods Appl. 2010; 73: 1783-91. https://doi.org/10.1016/j.na.2010.04.080

[38] Bosch M, Mukerji T, Gonzalez EF. Seismic inversion for reservoir properties combining statistical rock physics and geostatistics: A review. Geophysics. 2010; 75: 75A165-76. https://doi.org/10.1190/1.3478209

[39] Chi C, Mendel JM, Hampson D. A computationally fast approach to maximum-likelihood deconvolution. Geophysics. 1984; 49: 550-65. https://doi.org/10.1190/1.1441690

[40] Adeli H, Panakkat A. A probabilistic neural network for earthquake magnitude prediction. Neural Networks. 2009; 22: 1018-24. https://doi.org/10.1016/j.neunet.2009.05.003

[41] Pramanik AG, Singh V, Vig R, Srivastava AK, Tiwary DN. Estimation of effective porosity using geostatistics and multiattribute transforms: A case study. Geophysics. 2004; 69: 352-72. https://doi.org/10.1190/1.1707054

[42] Chambers R, Yarus J. Quantitative use of seismic attributes for reservoir characterization. CSEG Recorder. 2002; 27: 14-25.

[43] Singh S, Kanli AI, Sevgen S. A general approach for porosity estimation using artificial neural network method: a case study from Kansas gas field. Studia Geophysica et Geodaetica. 2016; 60: 130-40. https://doi.org/10.1007/s11200-015-0820-2

[44] De Bruin G, Bouanga EG. Time attributes of stratigraphic surfaces, analyzed in the structural and wheeler transformed domain. 69th EAGE Conference and Exhibition incorporating SPE EUROPEC 11-14 June. London, UK: European Association of Geoscientists & Engineers; 2007. https://doi.org/10.3997/2214-4609.201401624

[45] Aminzadeh F, De Groot P. Neural networks and other soft computing techniques with applications in the oil industry, Houten: Eage Publications; 2006.

[46] Henry S. Catch the (seismic) wavelet. AAPG Explorer 1997; 18: 36-8.

[47] Parzen E. On estimation of a probability density function and mode. Ann Math Stat. 1962; 33: 1065-76. https://doi.org/10.1214/aoms/1177704472

[48] Specht DF. Probabilistic neural networks. Neural Networks. 1990; 3: 109-18. https://doi.org/10.1016/0893-6080(90)90049-Q

[49] Specht DF. A general regression neural network. IEEE Trans Neural Netw. 1991; 2: 568-76. https://doi.org/10.1109/72.97934

[50] Muniz AMS, Liu H, Lyons KE, Pahwa R, Liu W, Nobre FF, *et al*. Comparison among probabilistic neural network, support vector machine and logistic regression for evaluating the effect of subthalamic stimulation in Parkinson disease on ground reaction force during gait. J Biomech. 2010; 43: 720-6. https://doi.org/10.1016/j.jbiomech.2009.10.018

[51] Maurya S, Singh N, Singh K. Seismic inversion methods: A practical approach. Springer Nature; 2020.

[52] Russell B, Hampson D. Comparison of poststack seismic inversion methods. 1991 SEG Annual Meeting, 1991, p. 876-8. https://doi.org/10.1190/1.1888870